

NUCLEAR DATA AND MEASUREMENTS SERIES

ANL/NDM-3
Neutron Scattering from Titanium:
Compound and Direct Effects

by

E. Barnard, J. deVilliers, P. Moldauer,
D. Reltmann, A. Smith, J. Whalen

October 1973

ARGONNE NATIONAL LABORATORY,
ARGONNE, ILLINOIS 60439, U.S.A.

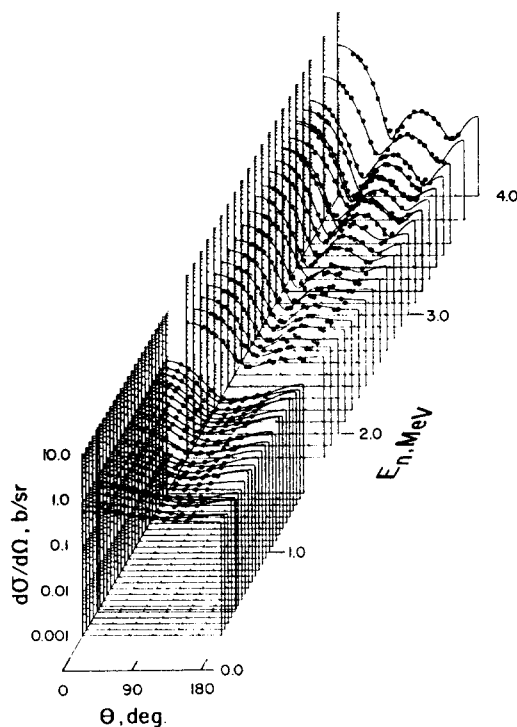
NUCLEAR DATA AND MEASUREMENTS SERIES

ANL/NDM-3
Neutron Scattering from Titanium;
Compound and Direct Effects*

by

E. Barnard,^a J. deVilliers,^a P. Moldauer,^b
D. Reitmann,^a A. Smith^b and J. Whalen^b

October 1, 1973



U of C - AUA - USAEC

ARGONNE NATIONAL LABORATORY,
ARGONNE, ILLINOIS 60439, U.S.A.

The facilities of Argonne National Laboratory are owned by the United States Government. Under the terms of a contract (W-31-109-Eng-38) between the U. S. Atomic Energy Commission, Argonne Universities Association and The University of Chicago, the University employs the staff and operates the Laboratory in accordance with policies and programs formulated, approved and reviewed by the Association.

MEMBERS OF ARGONNE UNIVERSITIES ASSOCIATION

The University of Arizona	Kansas State University	The Ohio State University
Carnegie-Mellon University	The University of Kansas	Ohio University
Case Western Reserve University	Loyola University	The Pennsylvania State University
The University of Chicago	Marquette University	Purdue University
University of Cincinnati	Michigan State University	Saint Louis University
Illinois Institute of Technology	The University of Michigan	Southern Illinois University
University of Illinois	University of Minnesota	The University of Texas at Austin
Indiana University	University of Missouri	Washington University
Iowa State University	Northwestern University	Wayne State University
The University of Iowa	University of Notre Dame	The University of Wisconsin

NOTICE

This report was prepared as an account of work sponsored by the United States Government. Neither the United States nor the United States Atomic Energy Commission, nor any of their employees, nor any of their contractors, subcontractors, or their employees, makes any warranty, express or implied, or assumes any legal liability or responsibility for the accuracy, completeness or usefulness of any information, apparatus, product or process disclosed, or represents that its use would not infringe privately-owned rights.

ANL/NDM-3
Neutron Scattering from Titanium;
Compound and Direct Effects*

by

E. Barnard,^a J. deVilliers,^a P. Moldauer,^b
D. Reitmann,^a A. Smith^b and J. Whalen^b

October 1, 1973

*This work supported by the South African Atomic Energy Board
and the U.S. Atomic Energy Commission.

^aPelindaba, Transvaal, Republic of South Africa.

^bArgonne National Laboratory, Argonne, Illinois, 60439, USA.

NUCLEAR DATA AND MEASUREMENTS SERIES

The Nuclear Data and Measurements Series presents results of studies in the field of microscopic nuclear data. The primary objective is the dissemination of information in the comprehensive form required for nuclear technology applications. This Series is devoted to: a) Measured microscopic nuclear parameters, b) Experimental techniques and facilities employed in data measurements, c) The analysis, correlation and interpretation of nuclear data, and d) The evaluation of nuclear data. Contributions to this Series are reviewed to assure a high technical excellence and, unless otherwise stated, the contents can be formally referenced. This Series does not supplant formal journal publication but it does provide the more extensive information required for technological applications (e.g. tabulated numerical data) in a timely manner.

TABLE OF CONTENTS

	<u>Page</u>
ABSTRACT	3
I. INTRODUCTION.	4
II. EXPERIMENTAL METHOD	5
III. EXPERIMENTAL RESULTS.	6
A. Total Neutron Cross Sections	6
B. Elastic Neutron Scattering Cross Sections.	6
C. Inelastic Neutron Scattering Cross Sections.	8
IV. DISCUSSION.	9
A. Optical Model and Statistical Calculations	9
B. Cross Section Fluctuations	12
V. MODIFICATION OF THE ENDF/B EVALUATED DATA FILE.	16
A. Total Neutron Cross Sections	17
B. Elastic Neutron Scattering Cross Sections.	17
C. Inelastic Neutron Scattering Cross Sections.	18
D. Other Exit Channels.	18
VI. SUMMARY	19

ANL/NDM-3

Neutron Scattering from Titanium;
Compound and Direct Effects

by

E. Barnard, J. deVilliers, P. Moldauer,
D. Reitmann, A. Smith and J. Whalen

ABSTRACT

Neutron total and elastic- and inelastic-scattering cross sections of natural titanium were measured. Total cross sections were determined from 0.1-1.5 MeV with resolutions of $\gtrsim 1.5$ keV. Differential elastic and inelastic neutron scattering cross sections were measured from 0.3-1.5 MeV with resolutions of $\gtrsim 10$ keV. The inelastic neutron excitation of states in ^{46}Ti (889 keV), ^{47}Ti (160 keV) and ^{48}Ti (984 keV) was observed. The energy-averaged behavior of the measured results was described in terms of spherical and ellipsoidal optical models and compound-nucleus and direct-reaction processes. The observed fluctuating cross sections were compared with the results of statistical R-matrix calculations based upon the energy-average model parameters and known resonance statistics. It was shown that both compound-nucleus and direct-reaction processes contribute to the fluctuating cross sections and that comparison of calculated and observed fluctuations gave an improved definition of the energy-average models. Furthermore the statistical R-matrix calculations displayed an intermediate resonance structure consistent with experimental observation without recourse to additional reaction mechanisms. The experimental results and their interpretations were used to improve the ENDF/B evaluated nuclear data file.

I. INTRODUCTION

Good resolution neutron cross sections of titanium to incident energies of ≈ 1.5 MeV are of interest in applied neutronic calculations and for their implications in basic nuclear physics.

Titanium is a potential structural material in applied neutronic systems particularly those based upon the fusion process and where weight is a consideration. Furthermore, an understanding of detailed resonance structure is critical to the calculation of deep neutron penetration through bulk media. The neutron energy range 0.1-1.5 MeV can be particularly difficult when the bulk material consists primarily of medium weight nuclei where the corresponding resonance structure is often not explicitly defined by experiments and therefore must be estimated from the statistical understanding of the processes.

The titanium isotopes lie in a region of large s-wave strength functions. The s- and d-wave widths of fast neutron resonances in titanium are relatively large. As a consequence, resonances in the energy range of the present study are expected to significantly overlap and interfere with one another. On the other hand, the number of open channels is small to incident neutron energies of 1.5 MeV and the average widths are not expected to be large compared to the resonance spacings. Therefore, the observed cross section fluctuations lie in a theoretically not well understood domain between isolated resonances and Ericson fluctuations [1]. It is of interest to study these fluctuations which arise from a few simultaneously interfering resonances and to ascertain to what extent they can be used to determine the statistical properties of resonance parameters and, in conjunction with energy-average cross sections, the optical model parameters.

Of further interest is the fact that the excitation of the first 2+ (0.984 MeV) state of ^{48}Ti by charged particle bombardment proceeds appreciably through direct excitation of the vibrational

properties of the nucleus [2]. A detailed examination of the high resolution neutron cross sections should reveal a similar direct component in the neutron induced processes.

For the above reasons neutron total and elastic and inelastic scattering cross sections have been measured in the incident neutron energy interval 0.1-1.5 MeV with particular attention to cross section definition and energy resolution. The results were compared with the predictions of optical and coupled-channel models of the energy-average cross sections. The observed cross section fluctuations were compared with those calculated from a statistical R-matrix model generated from spherical optical and coupled-channel model parameters. The experimental results and the associated physical interpretations were utilized to improve the widely used ENDF/B [3] evaluated nuclear data file.

II. EXPERIMENTAL METHODS

The experimental samples were cylinders of high purity natural titanium metal with neutrons incident on the bases or lateral surfaces in the total cross section or scattering measurements, respectively. All cross sections were determined in the units of barns per atom of the natural element.

The total neutron cross sections were deduced from the measured neutron transmissions through the samples. Both monoenergetic and pseudo-white source techniques were employed [4]. Attention was given to backgrounds and other experimental perturbations in order to minimize their effects. The validity of the experimental method was verified by determining the well-known total neutron cross sections of carbon [5].

All of the elastic and inelastic neutron scattering measurements employed fast neutron time-of-flight techniques [6] and all scattering cross sections were determined relative to the known differential elastic scattering cross sections of carbon [7]. The measured results were corrected for incident beam attenuation and multiple-event effects using Monte Carlo calculational procedures [8].

The total cross section, elastic scattering and "broad" resolution inelastic scattering measurements were made at Argonne. The "good" resolution inelastic neutron scattering cross sections were determined at Pelindaba. The details of the apparatus employed at the two laboratories are given in Ref. 9.

III. EXPERIMENTAL RESULTS

A. Total Neutron Cross Sections

Total neutron cross sections were determined from monoenergetic source measurements over the neutron energy ranges 0.1-0.45 MeV and 1.025-1.475 MeV with incident energy resolutions of ≈ 2 keV. The absolute energy scale was determined from known reaction thresholds (e.g. the ${}^7\text{Li}(p,n){}^7\text{Be}$ reaction) with an estimated uncertainty of ± 3 keV. Pseudo-white source time-of-flight techniques were employed over the energy range 0.45-1.025 MeV with velocity resolutions of ≈ 0.1 nsec/meter. The energy scale of the time-of-flight measurements was determined from a comparison of the neutron velocity with that of light with an estimated neutron energy uncertainty of ≈ 5 keV. The measured results are graphically summarized in Fig. 1.^a The estimated magnitude uncertainties in the measured total cross sections were 1-3%. The present results were consistent with previously reported values [10-12] but displayed more structure due to improved experimental energy resolutions. Resonances were evidently interfering when from a single isotope and overlapping when from various isotopes. When energy-averaged over intervals of ≈ 50 keV the observed total cross sections tended to display an intermediate resonance structure.

B. Elastic Neutron Scattering Cross Sections

Differential elastic scattering cross sections were measured at incident energy intervals of ≈ 20 keV from 0.3-1.5 MeV and at 8-10 scattering angles approximately equally distributed between

^aNumerical tabulations of all the experimental results reported herein can be obtained from the National Neutron Cross Section Center, Brookhaven National Laboratory [36].

25 and 155 degrees. The incident neutron resolution was ≈ 20 keV and the scattered neutron resolution sufficient to resolve the elastic contribution from all reported inelastic components. The measurements were made in a random manner over a period of six years using both single-detector and ten-detector systems. With the latter apparatus measurements made at different scattering angles employed independent measurement systems. The measured differential cross sections were least-square fitted with the expression

$$\frac{d\sigma}{d\Omega} = \frac{\sigma}{4\pi} \left(1 + \sum_{n=1}^4 W_n P_n \right) \quad (1)$$

where σ (the elastic cross section) and W_n coefficients were deduced from the fitting procedure and the P_n were Legendre polynomials expressed in the laboratory coordinate system. The fitting procedure was based only on the measured data with no additional constraints. The uncertainties in the measured differential cross sections were estimated to be $\approx 15\%$ and those of the angle-integrated elastic scattering cross sections $\approx 8\%$. These estimates were inclusive of systematic effects such as those associated with the carbon reference standard. The fit of Eq.(1) was descriptive of the measured values throughout the measured angular range and results obtained at slightly different scattering angles and/or incident energies were readily comparable when expressed in the format of Eq.(1). However, the fitted curve should be used with caution when extrapolating the experimental values beyond the measured angular interval though the fits were generally consistent with "Wick's Limit" [13] and extrapolated to reasonable 180° values.

The measured differential elastic scattering cross sections are summarized in the three-dimensional plot of Fig. 2. It is evident from the figure that the observed angular distributions fluctuated considerably with energy as expected from the resonance structure shown in Fig. 1. The angle-integrated elastic scattering cross sections deduced from the fitting of Eq.(1) were

consistent with the measured total cross sections when the variations in energy resolution, small uncertainties in energy scale and the presence of inelastic contributions were considered as indicated in Fig. 1. Comparable previous measurements of elastic neutron scattering from titanium were largely obtained at energies near 1.0 MeV. Some of these values are compared with the results of the present work in Fig. 3. In making this comparison the present values were averaged over the incident neutron energy range 0.9-1.1 MeV in order to reduce perturbations from resonance structure and possible differences in experimental energy resolution. The present work is in good agreement with that of Walt and Barschall [14] and, below the inelastic scattering thresholds, with the total neutron scattering angular distributions of Langsdorf et al. [7]. The agreement with the values given in Refs. 15 and 16 is less satisfactory.

C. Inelastic Neutron Scattering Cross Sections

Natural titanium consists of the even isotopes 46 (7.93%), 48 (73.94%) and 50 (5.34%) and the odd isotopes 47 (7.28%) and 49 (5.51%). Of these, titanium 46, 47 and 48 had reported states that could be readily excited by inelastic neutron scattering in the present experiments [2]. The observed excitation of states at 889.2 ± 0.2 keV and at 983.5 ± 0.2 keV was attributed to known $2+$ states in titanium 46 and 48, respectively. In addition, the observed excitation of a 159.6 ± 0.2 keV state was associated with the reported 160 keV ($\frac{7}{2}^-$) state in titanium 47. The energies of the states were established by the measurement of the gamma-rays emitted subsequent to inelastic neutron scattering with a calibrated GeLi detector [17]. The neutron cross sections for the excitation of the 159.6 keV state were small ($\lesssim 3$ mb/sr) and as a consequence were not reliably determined. Neutrons associated with the excitation of the 889.2 and 983.5 keV states were prominently observed and the corresponding cross sections quantitatively determined.

The angular distributions of inelastically scattered neutrons were determined with "broad" incident-energy resolutions of ≈ 20 keV. Generally these distributions were symmetric about 90° and nearly isotropic as illustrated in Fig. 4. Differential inelastic cross sections were determined with "good" incident energy resolutions (≈ 10 keV) at the single scattering angle of 90° . Angle-integrated inelastic neutron scattering cross sections were largely determined from a simple average of the measured differential values multiplied by 4π . In a few cases of appreciable anisotropy a fit of Eq.(1) to the measured values was used to determine the angle-integrated quantities. The uncertainty of the measured differential inelastic cross sections varied from measurement to measurement but generally was $\leq 10\%$ or 3 mb, whichever was larger. These uncertainty estimates were inclusive of systematic effects. The measured angle-integrated inelastic neutron scattering cross sections are summarized in Fig. 5. The "broad" and "good" resolution results were generally consistent within the respective experimental uncertainties though the latter show much more structure. In some instances there appeared to be a small difference between the energy scales of the two sets of measurements which were made at widely separated laboratories. Where these differences exist the calibration of the "good" resolution results was preferred as they were obtained in a more systematic manner.

Previously reported inelastic neutron scattering cross sections of titanium in the energy range of the present experiments are sparse. However, the non-elastic scattering results obtained by Beyster et al. [18] near 1.0 MeV are consistent with the total inelastic scattering cross section derived from the present experiments.

IV. DISCUSSION

A. Optical Model and Statistical Calculations

The experimental values were compared with those calculated from optical-model and statistical theories [19,20]. The majority of the calculations employed a spherical potential consisting of:

a Saxon-Woods real term, a Gaussian surface-imaginary term and a Thomas spin-orbit term [21]. Non-locality was approximated by the use of energy dependent parameters [22]. The effects of direct-reactions were examined using an ellipsoidal potential inclusive of two-channel coupling of ground and first excited states of the even isotopes [23].

An initial estimate of the spherical potential parameters was obtained from a comparison of energy-averaged measured and calculated total neutron cross sections. Subsequent small adjustments were made to achieve an acceptable description of the observed elastic neutron scattering angular distributions inclusive of compound-nucleus contributions. Inelastic neutron scattering cross sections were not utilized in the selection of the optical potential. The parameter adjustments included real and imaginary potential strengths, radii and diffusenesses. The final choice was based upon subjective judgement. Numerical procedures, such as χ -square fitting, tended to result in parameters only descriptive of energy-local structure and not particularly suitable over the entire experimental range. The resulting "selected" parameter set, given in Table 1, was based entirely upon comparisons with the present experimental results.

All of the measured cross sections displayed large fluctuations which remained appreciable even after averaging over 200 keV. Thus the agreement between calculated total and elastic scattering cross sections and the measured values varies with energy as shown in Figs. 1, 3 and 4. However, in the context of the entire experimental energy range, the model provides a good description of both the measured total cross sections and the elastic scattering angular distributions.

Inelastic neutron scattering cross sections were calculated using the Hauser-Feshbach formula [20] and the above "selected" spherical potential. The calculations included the excitation of states at 160 (^{47}Ti), 889 (^{46}Ti) and 984 (^{48}Ti) keV assuming the latter two were $2+$ states and the former a $\frac{7}{2}$ - state [2].

The calculated cross section for the excitation of the 160 keV state, corrected for isotopic abundance, was consistent with the marginal experimental observation. The calculated excitation of the 984 keV state, indicated by the "Spherical Model #1" curve of Fig. 5, compared favorably with the energy average of the measured values. Similar agreement was achieved between measured and calculated excitations of the 889 keV state. Calculated inelastic neutron angular distributions were nearly isotropic, as illustrated in Fig. 4, and reasonably consistent with the experimental observation.

The even-isotopes of titanium are deformed with 2+ vibrational first excited states. Of these the 984 keV state in ^{48}Ti was the major contributor to the observed inelastic neutron scattering. The effect of the deformation on the inelastic excitation of these vibrational states was examined using an ellipsoidal optical potential with two-channel coupling and a $\beta_2 = 0.25$ [23]. Generally, the elastic angular distributions calculated with the ellipsoidal form of the "selected" potential of Table 1 were in somewhat better agreement with the measured values than those obtained from the spherical calculations. This is illustrated by the curves of Fig. 3 (and, to a lesser extent, Fig. 4). The inelastic neutron scattering cross sections calculated from the ellipsoidal potential were larger than those obtained from the spherical calculations and in somewhat better agreement with the measured values as illustrated by the curves of Figs. 4 and 5. The inelastic neutron angular distributions calculated from the ellipsoidal potential were slightly asymmetric about 90° (a few mb/sr) but not sufficiently so to be observed in the present experiments. Generally, the fluctuating nature of the inelastic scattering cross sections observed in the present experiments tended to mask the relatively small differences between values calculated with spherical and ellipsoidal potentials. This was not true of the statistical analysis of the fluctuations described in Sec. IV-B, below.

Elastic scattering angular distributions calculated from the "selected" potential were consistent with previously reported measurements at 3.2 and 4.1 MeV [24,25] particularly when the ellipsoidal potential form was used. Calculated total neutron cross sections were in good agreement with reported experimental values to energies of 5.0 MeV [26] but then became smaller than the measured values with increasing energy amounting to a discrepancy of 10-15% at 10.0 MeV. The calculated inelastic scattering cross sections were sensitive to the choice of model. For example, the general potential of Moldauer [27] (PAM of Table 1) and the Hauser-Feshbach formula lead to calculated values appreciably larger than measured quantities as illustrated by the "Spherical Model #2" curve of Fig. 5. Furthermore, the importance of resonance width fluctuation corrections in the region of titanium has been pointed out [28] and there is a small resonance interference factor. When these "corrections" were applied to the PAM results a good agreement with measured inelastic scattering cross sections was achieved as illustrated by the "Spherical Model #2 w/corrs" curve in Fig. 5 (and in Fig. 4). The upper of the two "corrected" curves in Fig. 5 corresponds to the parameter $Q = 0$, the lower to $Q = 1$ [28]. Similar application of fluctuation and correlation corrections to calculations based upon the "selected" potential generally resulted in inelastic scattering cross sections somewhat smaller than those observed experimentally. Thus, in the context of the measured inelastic neutron scattering cross sections, the choice of potential was appreciably influenced by the nature of the corrections applied to the Hauser-Feshbach formula. Such corrections had a much smaller effect on the calculated elastic neutron scattering cross sections, thus did not strongly influence the above potential selection which was based upon comparisons of measured and calculated neutron total and elastic scattering cross sections.

B. Cross Section Fluctuations

In the above only energy-averages of measured cross sections have been interpreted in terms of theoretical parameters. The observed values strongly fluctuate and the analysis of

these fluctuations confirm the theoretical basis for the calculation of energy-averaged cross sections and provide a check on the validity of the optical model parameters. In addition, the fluctuation analysis provides information on level densities, tests the validity of the experimental energy resolution and provides a statistical "synthetic" cross section of "infinitely-good" resolution suitable for applied neutron physics calculations. The analytical procedure is to calculate the energy-dependence of the cross sections on the basis of optical- and statistical-model information applied to R-matrix theory [29]. The procedure, which has been described in detail elsewhere [30], is briefly as follows.

In the absence of direct reactions, the optical model channel amplitudes $\eta_{\alpha,\ell,j}$ specify the R-matrix parameters R^∞ , $\langle \gamma^2 \rangle / D$ through

$$R_{\alpha,\ell,j}^\infty + i\pi \langle \gamma_{\alpha,\ell,j}^2 \rangle / D = \frac{1 - \eta_{\alpha,\ell,j} \exp(2i\phi_{\alpha,\ell,j})}{L_{\alpha,\ell,j}^* - L_{\alpha,\ell,j} \eta_{\alpha,\ell,j} \exp(2i\phi_{\alpha,\ell,j})} \quad (2)$$

where α specifies an elastic or inelastic exit channel, ℓ the orbital neutron angular momentum and j the total neutron angular momentum. The remaining quantities of Eq.(2) are well known from R-matrix theory. The next step is to construct a statistical R-matrix with elements

$$R_{\alpha\ell j, \alpha'\ell'j'} = R_{\alpha\ell j}^\infty \delta_{\alpha\alpha'} \delta_{\ell\ell'} \delta_{jj'} + \sum_{\mu} \frac{\gamma_{\mu\alpha\ell j} \gamma_{\mu\alpha'\ell'j'}}{E_{\mu} - E} \quad (3)$$

where level energies E_{μ} are chosen at random to satisfy the Wigner distribution of level spacings and a mean spacing D which is in accord with the spacings of neutron resonances and with the theory of the angular momentum and energy dependence of the level density. The real quantities $\gamma_{\mu\alpha\ell j}$ are chosen at random to be normally distributed about the mean, to be statistically independent for different values of $\alpha\ell j$ and so that the level average $\langle \gamma_{\mu\alpha\ell j}^2 \rangle_{\mu}$ has the value required by Eq.(2). From the statistical R-matrix of Eq.(3) we can calculate statistical S-matrix elements and statistical cross sections in the usual R-matrix manner.

If some channels are coupled by a direct reaction, such as is the case for the ground and first excited states in the even titanium isotopes, then the optical model amplitudes $\eta_{\alpha, \ell, j}$ in Eq.(2) must be replaced by a coupled-channel matrix of amplitudes with non-vanishing elements between directly coupled channels. In that case Eq.(2) is replaced by a matrix equation which specifies an R^∞ matrix having off-diagonal elements. This matrix equation also specifies non-vanishing values for $\langle \gamma_{\mu\alpha\ell j} \gamma_{\mu\alpha'\ell'j'} \rangle_\mu$ when these two channels are directly coupled. Thus the random R-matrix γ 's must now be chosen so as to have the indicated correlation between directly coupled channels. Except for these complications the calculation proceeds exactly as in the case of purely compound-nucleus reactions.

The above computational procedures have been incorporated in a computer program STASIG [31]. A random number generator is used to select the R-matrix parameters $\gamma_{\mu, \alpha, \ell, j}$ and E_μ in accordance with the optical- and statistical-model and the appropriate statistical cross sections are calculated. These calculated cross sections are then averaged using a flat resolution function with Gaussian fall-off at the edges corresponding to the experimental energy resolution. The result of the calculation is then statistically comparable with the respective experimental values. Of course, only statistical comparisons such as are provided by auto-correlation functions and the general character of the fluctuations are significant. The internal consistency of the calculational procedure can be verified by averaging the statistical result over large energy intervals thereby deducing average cross section values which must be consistent with those calculated directly from the optical model used as an input to the statistical calculations. The neutron total and inelastic scattering cross sections of the even isotopes of titanium were calculated following the above principles using both ellipsoidal and spherical models. The calculated total neutron cross sections are compared with the experimental values in Figs. 6 and 7. In making these comparisons the calculated results

were energy-broadened to yield a "resolution" equivalent to that of the experiments using the resolution function outlined above. Qualitatively, the ellipsoidal calculation gives a better description of the measured values than does the spherical calculation particularly with respect to the extrema of the structure and the trend toward grouping of resonances. The comparisons may indicate that the experimental resolution was not as good as believed. The character of the broad maxima evident in the ellipsoidal calculations is dependent upon the statistical nature of the particular calculation and will change in detail but not in gross features.

Similar comparisons of measured and calculated cross sections for the excitation of the 984 keV state in ^{48}Ti are shown in Fig. 8. In these comparisons the "resolution" introduced into the calculations was 12-15 keV. The result obtained with the ellipsoidal calculation is very similar to the measured values with the same general statistical magnitudes and structures. In particular, the minima of the structure are in reasonable agreement with the experimental values. In contrast, the results obtained with the spherical calculation do not describe the experimental results well either in magnitude or in gross features of the structure.

When averaged over wide energy increments the results of the statistical calculation should reduce to the optical model result upon which it was based. This is illustrated in Fig. 9 which compares the ellipsoidal optical model results with the 100 keV energy-averages of the ellipsoidal statistical calculations and the experiments. The averages are consistent. Similar consistency can be obtained using the spherical model which, as noted above, does not lead to statistical fluctuating cross sections particularly descriptive of experiment. Thus the fluctuations of the statistical calculations can provide a sensitive test of the suitability of the optical potential.

The comparisons of Figs. 6-8 can be put on a more quantitative basis by means of auto-correlation functions. Fig. 10 shows auto-correlation distributions derived from the measured total neutron cross sections and those calculated with both ellipsoidal

and spherical statistical models. The distributions obtained from the experiments and the ellipsoidal calculations are very similar particularly with respect to magnitudes and average widths. The auto-correlation function derived from the results of the spherical calculation is very different in general character and in magnitude.

The comparison of the statistical model calculational results with the fluctuating measured cross sections is a more sensitive test of the optical-coupled-channels-model description than is a comparison with the average measured cross sections. Comparison of statistical cross section fluctuations with experimental results gives an indication of true experimental resolution. The latter may tend to be optimistic, as apparently is so in the present context. The ellipsoidal calculations result as an intermediate resonance effect similar to that evident in the experiments without recourse to additional reaction mechanisms. The statistical results can be of considerable applied interest as they indicate the "true" magnitudes of the fluctuating structure important to some applications (e.g. neutron transport through bulk media) in a manner not easily obtainable experimentally, if at all.

V. MODIFICATION OF THE ENDF/B EVALUATED DATA FILE

The Evaluated Nuclear Data File-B (ENDF/B) contains titanium, MAT-1016 [3]. This evaluation was prepared by Pennington and was largely based upon prior evaluated data sets. In order to make available the results of the present work and other recent experimental values in a readily usable form the titanium ENDF/B file was modified and updated. The revised file has been transmitted to the NNCSC [32]. The following discussion outlines the procedures used in the revision and the scope of the modifications.

The modifications were confined to incident neutron energies above 0.1 MeV. Values at all lower incident energies were explicitly retained in the original form. The modification emphasized

experimental values and used the model-calculations outlined above to extrapolate the measured quantities where necessary. The file requires internal consistency which is not available in detail from the experimental values primarily due to the different experimental resolutions employed in the various measurements. Thus construction of the file requires appreciable extrapolation and interpolation of measurements. Generally, the procedures used in the modification were as follows.

A. Total Neutron Cross Sections

Total cross section values in the energy range 0.1-1.5 MeV were taken explicitly from the experimental results of the present work. From 1.5-10.0 the experimental values from the works of Schwartz [10], Barschall et al. [33] and Foster and Glasgow [34] were used. Above 10.0 MeV the measured values were extrapolated with model calculations using the potential described above normalized to experimental values at 10.0 MeV. Where necessary the measured total cross sections were linearly interpolated in energy so as to assure that the energies of the partial cross sections were a sub-set of the total cross section energies. The resulting total cross section is indicated in Fig. 11.

B. Elastic Neutron Scattering Cross Sections

The elastic scattering cross section was calculated directly from the evaluated total cross section (above) and the non-elastic scattering cross section. The non-elastic cross section was constructed from the various partial cross sections and linearly interpolated to the more detailed energies of the total cross section file. Where necessary partial cross sections of ENDF/B, MAT-1016 were used. In this manner, the resulting evaluated elastic cross section retained the detail of the high-resolution total cross section file and maintained internal consistency. When averaged over corresponding energy increments the evaluated elastic scattering cross sections were in good agreement with those measured in the present work. The resulting elastic scattering cross section of the modified file is shown in Fig. 11.

The elastic scattering angular distributions were expressed as $f_{\ell}(E)$ coefficients as defined by the ENDF/B format. At neutron energies of ≤ 1.5 MeV these coefficients were taken explicitly from the present experimental results. Additional experimental results were used at 3.2 MeV [24] and 4.0 MeV [25]. Model-calculations, normalized to available experimental values, were used to interpolate the measurements and extrapolate the $f_{\ell}(E)$ coefficients to higher energies. The $f_{\ell}(E)$ values obtained in the above manner provide a good representation of the available experimental information. However, they are generally based upon measurements with approximately an order of magnitude poorer resolution than that employed in total cross section studies. Thus $f_{\ell}(E)$ values will not display the detailed energy dependent structure of either the total or elastic cross sections of the file.

C. Inelastic Neutron Scattering Cross Sections

The inelastic neutron scattering cross sections were assumed to be entirely due to the even isotopes of titanium (87% abundance). At incident neutron energies of ≤ 1.5 MeV the experimental results of the present work were explicitly used. These components plus the cross sections due to the excitation of known states at 2.32, 2.40 and 3.2 MeV [2] were extrapolated to incident neutron energies of ~ 7.0 MeV guided by calculations including qualitative estimates of the contribution from the inelastic continuum. At higher energies the continuum inelastic distributions and nuclear temperatures of the original evaluation were retained. The resulting partial and total inelastic neutron scattering cross sections are shown in Fig. 12.

D. Other Exit Channels

Radiative capture cross sections, $(n;\chi)$ reaction cross sections where $\chi \neq$ neutron and $(n;2n)$ cross sections were retained from the original evaluation without modification as the present experimental results did not directly define these quantities. These reaction cross sections were incorporated in the non-elastic cross section utilized in the derivation of the elastic cross section outlined above. Where necessary various partial cross sections were interpolated in energy and magnitude in a linear manner.

The revised ENDF/B file deduced in the above manner was verified with respect to "housekeeping" errors using the check routine . CHECKER [32] and the physical content inspected with various ad-hoc graphical procedures. The final result was transmitted to the NNCS [32] with the objective of significantly improving the titanium-ENDF/B file at energies above 0.1 MeV.

VI. SUMMARY

The experimental results provide an improved basis for the physical interpretation and applied use of fast neutron interactions with titanium particularly including total and scattering cross sections to 1.5 MeV.

The energy-averaged experimental cross sections were well described by either spherical or ellipsoidal optical models and the Hauser-Feshbach formula. The choice of model is not unique and the resonance fluctuation and correlation corrections to the Hauser-Feshbach formula introduce further ambiguities.

A statistical R-matrix based upon energy-averaged model parameters and the known statistical properties of resonances was used to calculate the detailed statistical fluctuations of the total and scattering cross sections. The calculated results were sensitive to the choice of the energy-averaged model and comparison with the experimental results indicates the importance of the ellipsoidal model and channel-coupling in the description of the cross section fluctuations. The statistical R-matrix calculations give an indication of intermediate resonance structure similar to that apparent in the experimental results without recourse to other reaction mechanisms. Furthermore, they give an independent indication of the actual experimental resolutions and provide the detailed statistical knowledge of the resonance structure essential to some applications and not generally directly available from experiment.

The experimental results and the associated interpretations were utilized to modify and improve the ENDF/B titanium data file particularly in the areas of fluctuating neutron total and elastic and inelastic scattering cross sections.

ACKNOWLEDGMENT

The authors wish to express their appreciation of assistance rendered by members of the Pelindaba and Argonne staffs in many facets of the work.

REFERENCES

1. T. Ericson and T. Mayer-Kuckuk, Ann. Rev. Nucl. Sci. 16 (1966) 183.
2. J. Rapaport, "Nuclear Data Sheets for A=48," p. 351 (1970) (see also 46 and 47).
3. Evaluated Nuclear Data File-B (ENDF/B) MAT-1064, National Neutron Cross Section Center, Brookhaven National Laboratory.
4. J. Whalen, Applied Physics Division Annual Report, Argonne National Laboratory (1972), in press.
5. S. Cierjacks, P. Forti, D. Kopsch, L. Kropp, J. Nebe and H. Unseld, Kernforschungszentrum Karlsruhe Report KFK-1000 (1968).
6. See for example, A. Smith, J. Whalen and P. Guenther, Applied Physics Report AP/CTR/TM-4, Argonne National Laboratory (1973).
7. A. Langsdorf, R. Lane and J. Monahan, Phys. Rev. 107 (1957) 1077.
8. A. Smith and P. Guenther, to be published.
9. E. Barnard, J. deVilliers, C. Engelbrecht, D. Reitmann and A. Smith, Nucl. Phys. A118 (1968) 321.
10. R. Schwartz, private communication (1972).
11. J. Garg, J. Rainwater and W. Havens, Jr., Bull. Am. Phys. Soc. 8 (1963) 334.
12. E. Bilpuch, K. Seth, C. Bowman, R. Tabony, R. Smith and H. Newson, Ann. Phys. 14 (1961) 387.
13. G. Wick, Phys. Rev. 75 1459 (1949).
14. M. Walt and H. Barschall, Phys. Rev. 93 (1954) 1062.
15. G. Lovchekova, Sov. J. Atom. Energy 12 (1962) 46.
16. S. Darden et al., Phys. Rev. 96 (1954) 836.
17. D. Smith, private communication.
18. J. Beyster, M. Walt and E. Salmi, Phys. Rev. 104 (1956) 1319.
19. H. Feshbach, C. Porter and V. Weisskopf, Phys. Rev. 96 (1954) 448.

20. W. Hauser and H. Feshbach, Phys. Rev. 87 (1952) 366.
21. P. Hodgson, "The Optical Model of Elastic Scattering," Clarendon Press, Oxford (1963).
22. C. Engelbrecht and H. Fiedeldey, Ann. Phys. 42 (1967) 262.
23. C. Dunford, Atomic International Report, NAA-SR-11706 (1966).
24. R. Becker, W. Guindon and G. Smith, Nucl. Phys. 89 (1966) 154.
25. J. Towle, private communication, Data from the National Neutron Cross Section Center, Brookhaven National Laboratory.
26. M. Goldberg, S. Mughabghab, B. Magurno and V. May, "Neutron Cross Sections, Vol. IIA, Supl. 2," Brookhaven National Lab. Report, BNL-325 (1966).
27. P. Moldauer, Nucl. Phys. 47 (1963) 65.
28. P. Moldauer, Rev. Mod. Phys. 36 (1964) 1079.
29. A. Lane and R. Thomas, Rev. Mod. Phys. 30 257 (1958).
30. P. Moldauer, "Statistical Properties of Nuclei," Conf. Proc. Ed., J. Garg, Plenum Pub. Co., New York, p. 335 (1972).
31. P. Moldauer, private communication.
32. National Neutron Cross Section Center (NNCSC), Brookhaven National Laboratory, Upton, New York.
33. A. Carlson and H. Barschall, Phys. Rev. 158 (1967) 1142.
34. D. Foster and D. Glasgow, Phys. Rev. C3 (1971) 576.

TABLE I. Optical Potential Parameters

Parameter	<u>Potential</u>	
	Selected	PAM
Real Well		
Depth, MeV	44.5	46.0
Radius, F	4.543	4.815
Diffuseness, F	0.62	0.62
Imaginary Well		
Depth, MeV	9.0	14.0
Radius, F	4.797	5.316
Diffuseness, F	0.50	0.50
Spin-Orbit		
Depth, MeV	7.0	7.0
Deformation Parameter ^b	0.252	---

^aApplicable only to the ellipsoidal calculations.

^bThe direct-well was set equal to the real-well.

FIGURE CAPTIONS

- Fig. 1. Measured neutron total (vertical bars) and angle-integrated elastic scattering (boxes) cross sections of titanium. The solid curve indicates the total cross section calculated from the "selected" potential of Table I and the dashed curve that calculated from the potential of Ref. 27.
- Fig. 2. Measured differential elastic neutron scattering cross sections of titanium. Experimental values are indicated by data points. The curves represent the fit of Eq.(1) to the measured values.
- Fig. 3. Comparison of measured and of calculated differential elastic neutron scattering cross sections of titanium near 1.0 MeV. The present experimental values are indicated by boxes. Other experimental results are shown by: (Ref. 14) and (Ref. 15). Results of optical model calculations are indicated as follows:
———— = calculated from the spherical "selected" potential of Table I, — — — = the ellipsoidal form of the "selected" potential, and — - - - = the spherical potential of Ref. 27.
- Fig. 4. Angular distributions of 1.4 MeV neutrons elastically and inelastically ($Q = -983.5$ keV) scattered from titanium. Measured values are indicated by data points. The results of optical statistical model calculations are indicated as follows; ————— = the "selected" spherical potential of Table I, — — — = the ellipsoidal form of the "selected" potential, and the — - — and — - - — curves the spherical potential of Ref. 27 with fluctuation corrections and the correlation parameter, Q , equal to 0 and 1, respectively.

Fig. 5. Cross sections for the inelastic neutron excitation of the 889.2 and 983.5 keV states in titanium. "Good" resolution results for the 983.5 keV state are indicated by circular data points (joined by dotted curve), those for the 889.2 keV state by crosses. "Broad" resolution results for the 983.5 keV state are indicated by boxes. Curves show calculational results based upon the following potentials: Model #1 is the "selected" potential of Table I in spherical (————) and ellipsoidal (— — —) forms. "Model #2" is the potential of Ref. 27 with the upper (— — —) curve giving the Hauser-Feshbach result and the two lower curves showing the same result corrected for resonance fluctuations and correlations as described in Sec. IV of the text.

Fig. 6. Comparison of measured and calculated total neutron cross sections of titanium in the energy range 0.5-1.0 MeV. The upper curve is obtained directly from the experimental values. The lower two curves indicate the results of statistical R-matrix calculations using ellipsoidal and spherical optical potentials energy-averaged over an energy resolution function equivalent to that of the experimental measurements.

Fig. 7. Comparison of measured and calculated total neutron cross sections of titanium in the energy range 1.0-1.5 MeV. The format is identical to that of Fig. 6.

Fig. 8. Comparison of measured and calculated elemental cross sections for the excitation of the 983.5 keV state in titanium. The upper curve indicates the "good" resolution experimental data. The lower two curves show the results of statistical R-matrix calculations based upon ellipsoidal and spherical optical potentials energy-averaged over a resolution function approximating that of the experiments.

- Fig. 9. Comparison of the total neutron cross sections of titanium obtained from: a 100 keV energy-average of the experimental results, a similar average of the results of statistical R-matrix calculations based upon an ellipsoidal potential, and from the ellipsoidal optical potential employed in the statistical calculations.
- Fig. 10. Comparison of auto-correlation distributions obtained from the total neutron cross sections as: determined experimentally, calculated with a statistical R-matrix based upon an ellipsoidal potential and as similarly calculated from a spherical potential.
- Fig. 11. Evaluated neutron total and elastic scattering cross sections of titanium over the energy range 0.1-18.0 MeV.
- Fig. 12. Evaluated partial cross sections of titanium over the energy range 0.01-18.0 MeV.

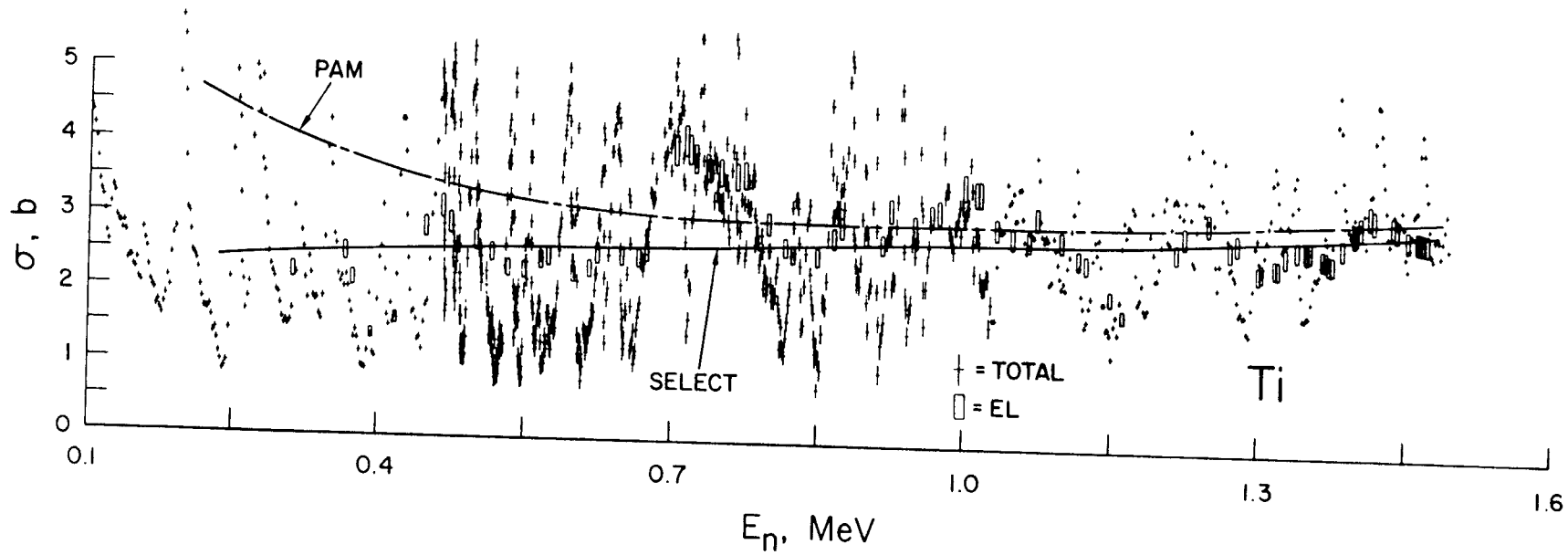
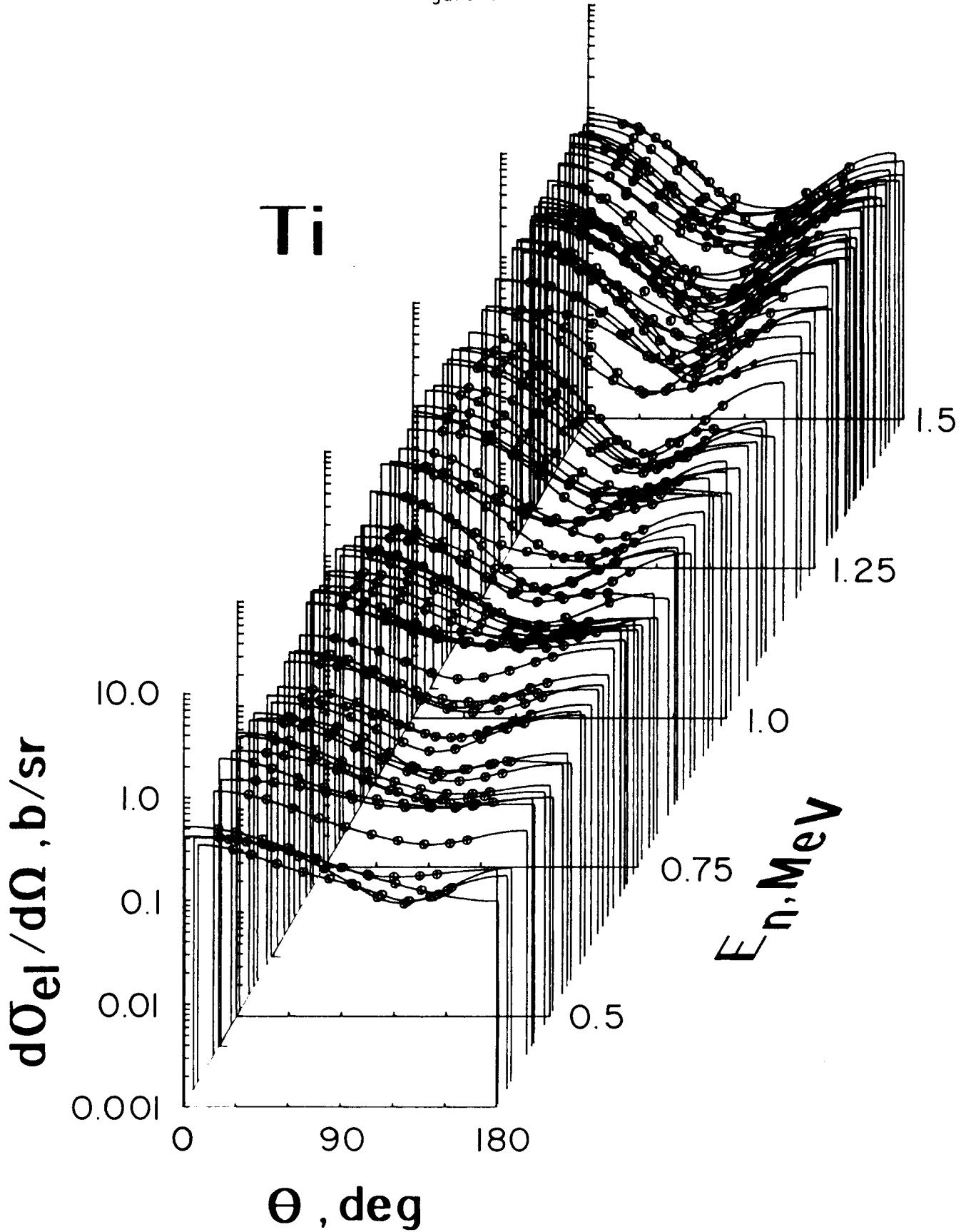


Figure 1

Figure 2



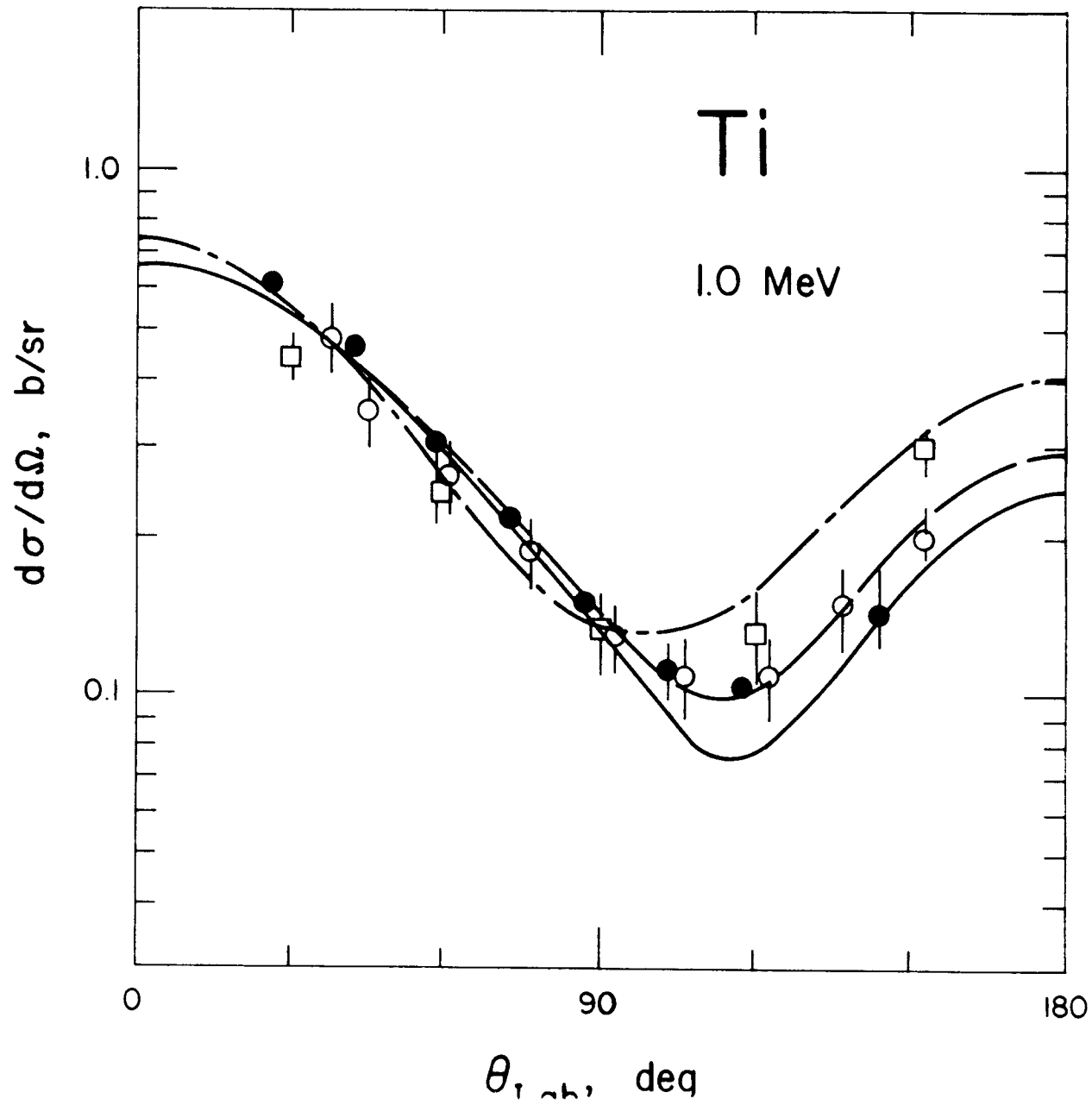
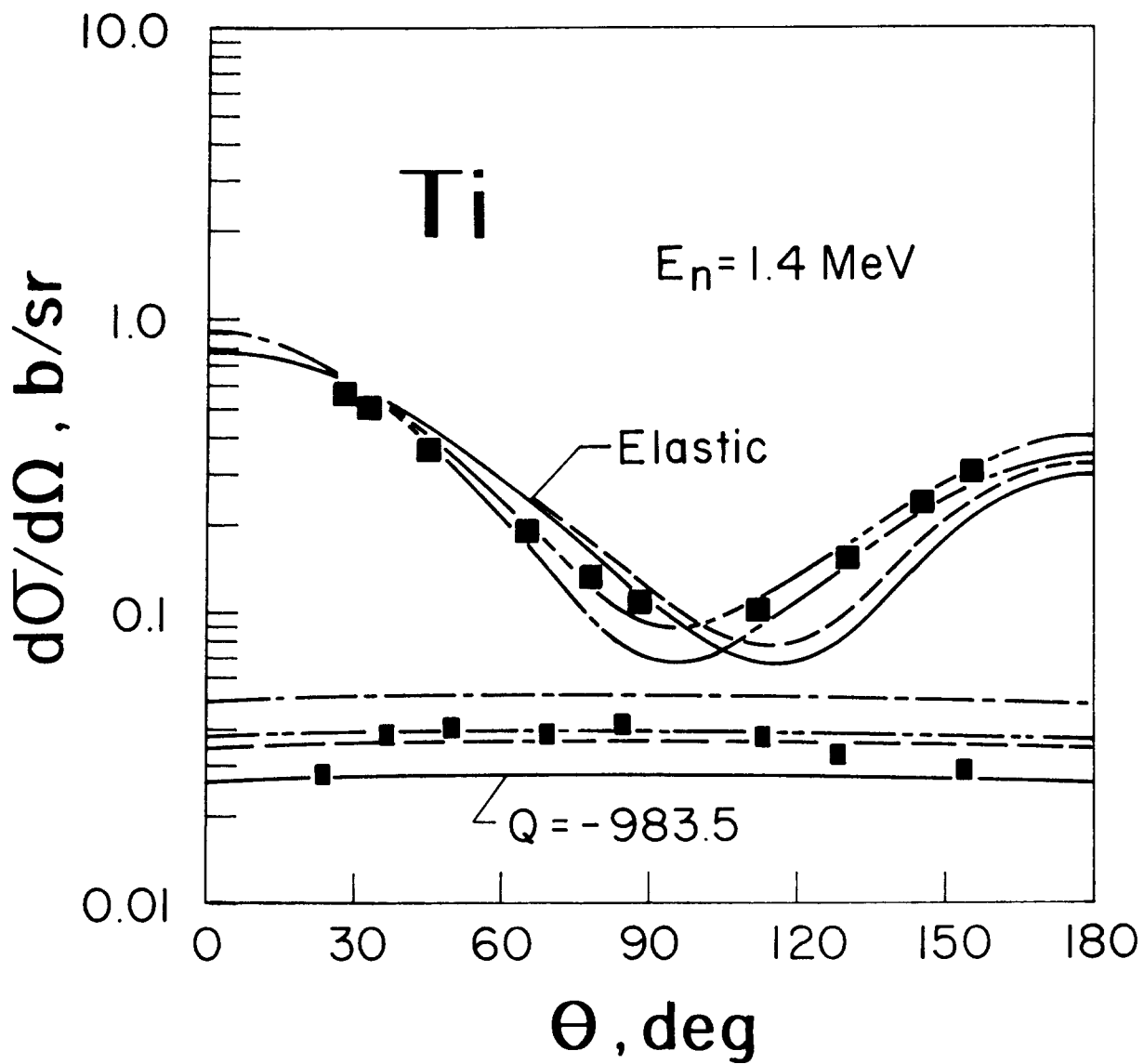


Figure 3

Figure 4



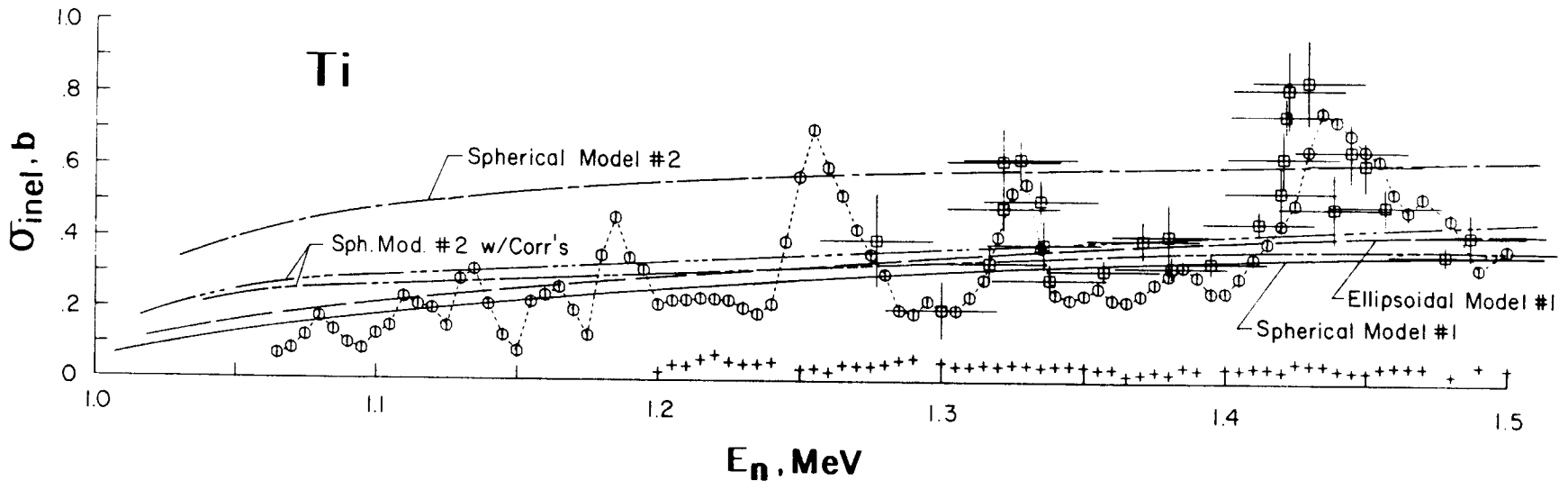


Figure 5

Figure 6

Ti

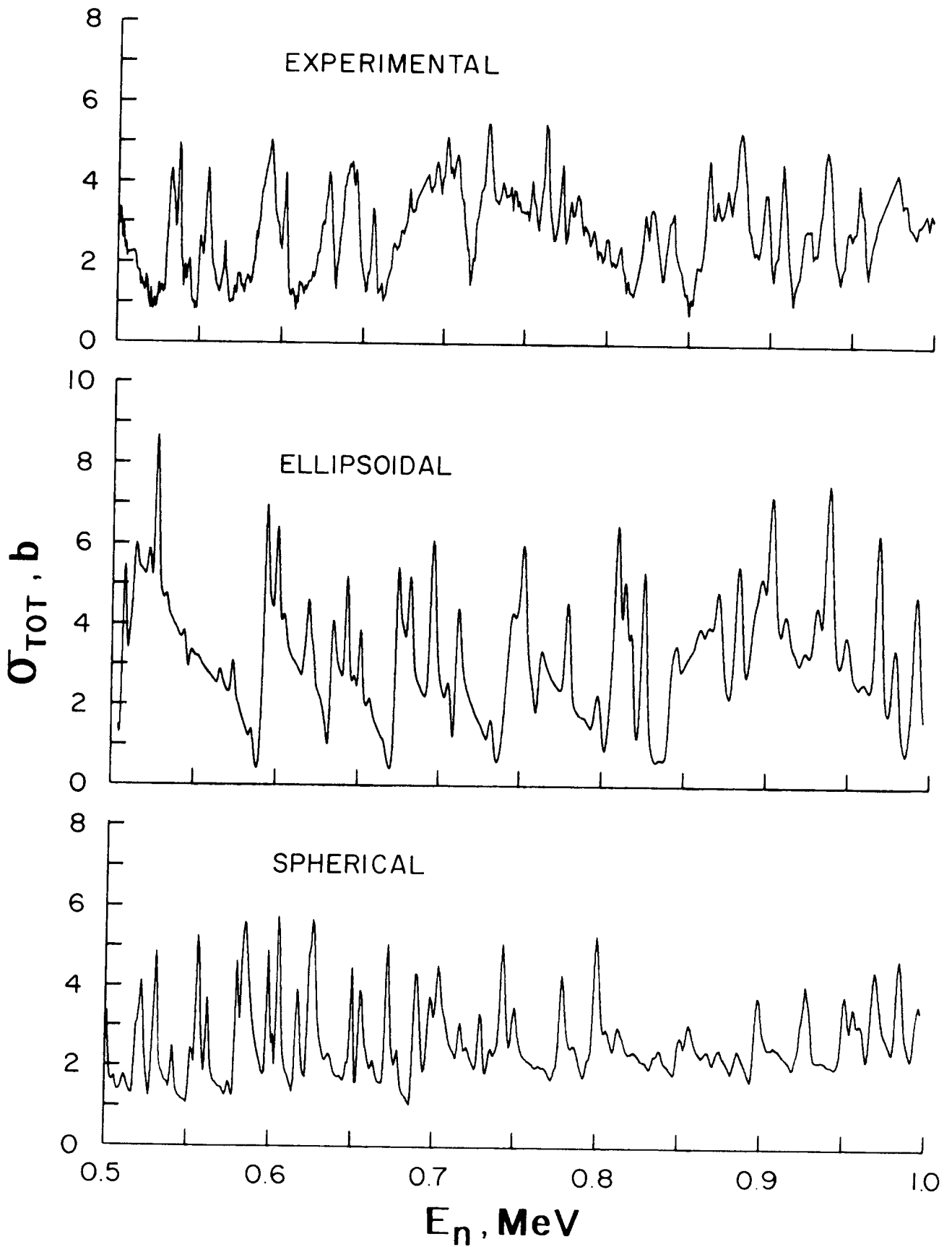


Figure 7

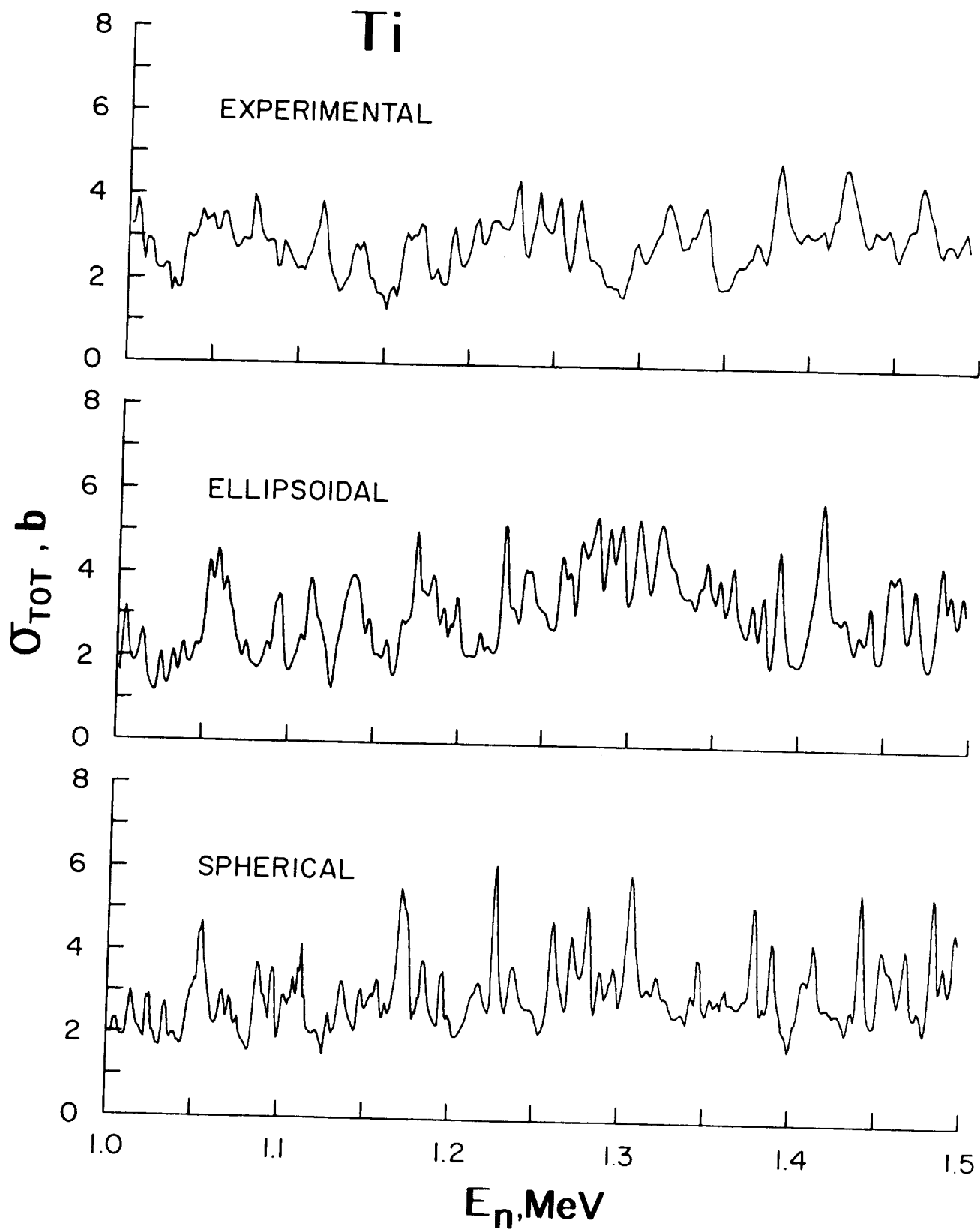
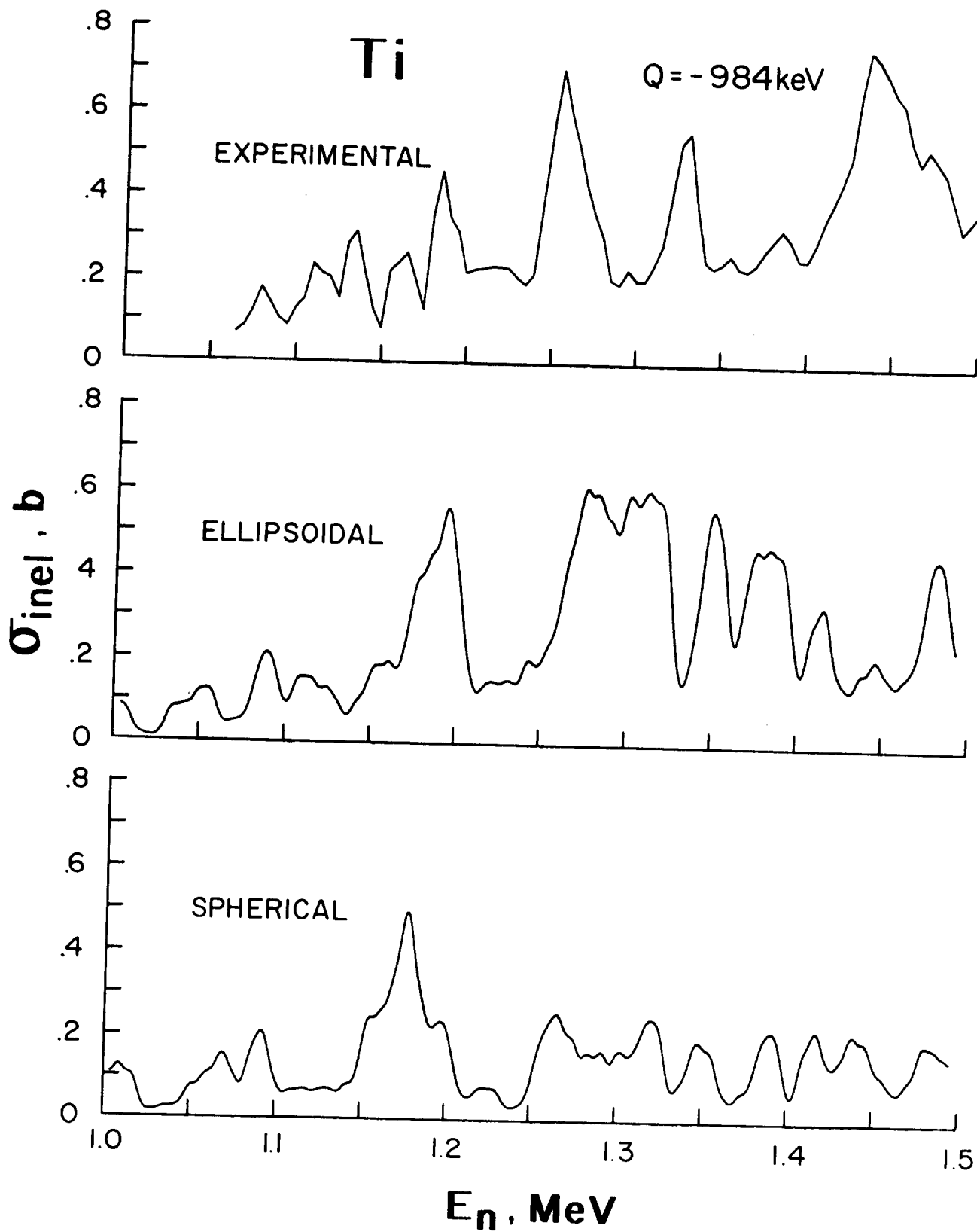


Figure 8



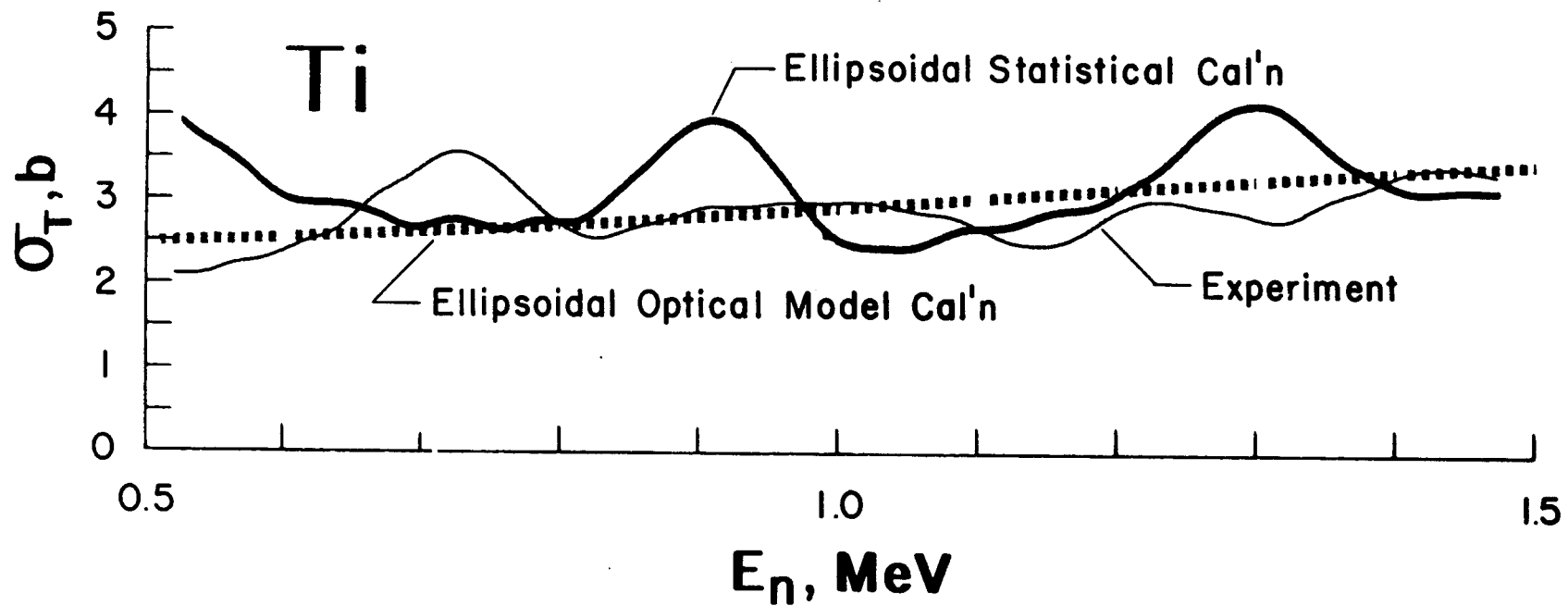
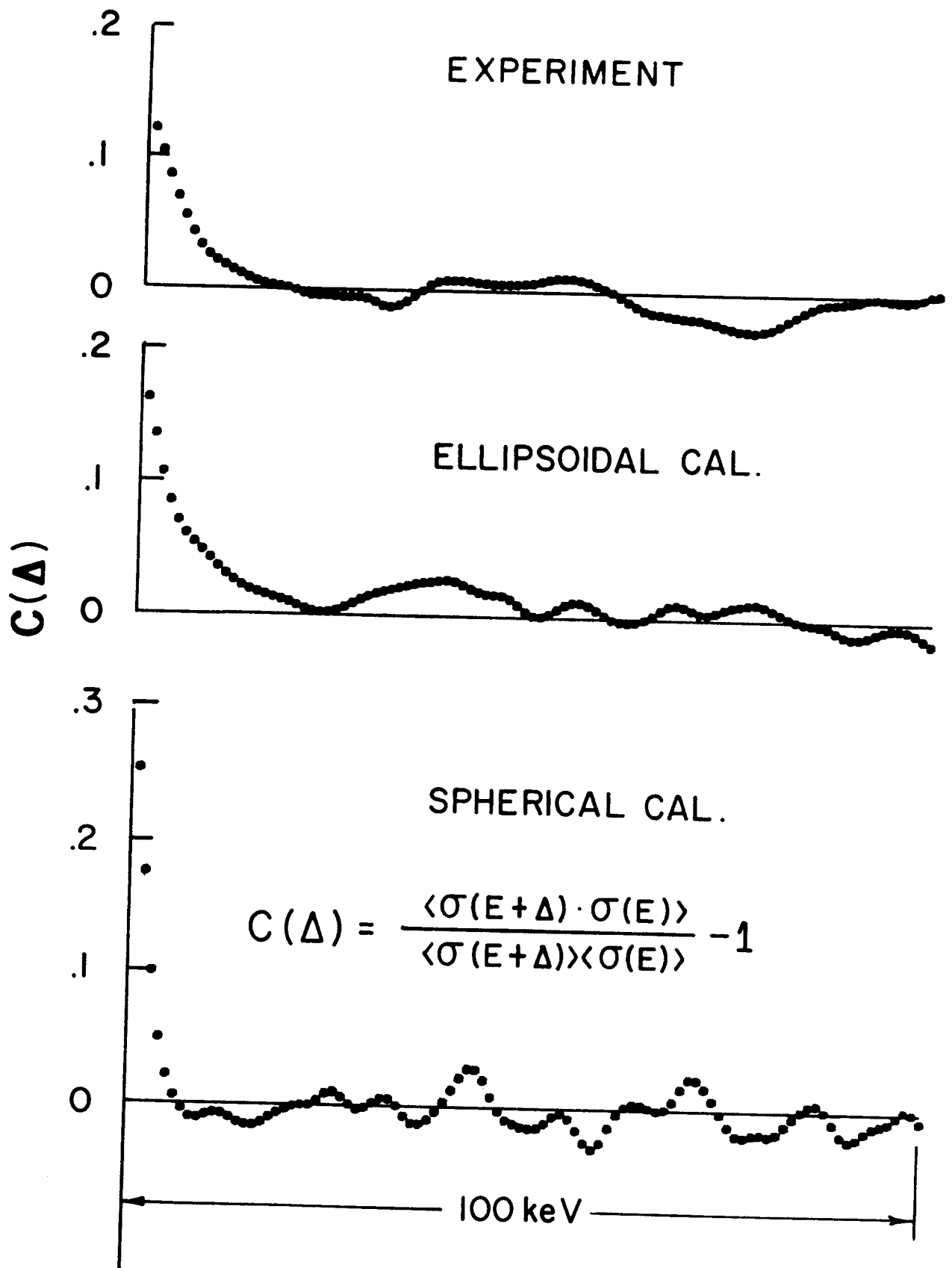


Figure 9

Figure 10



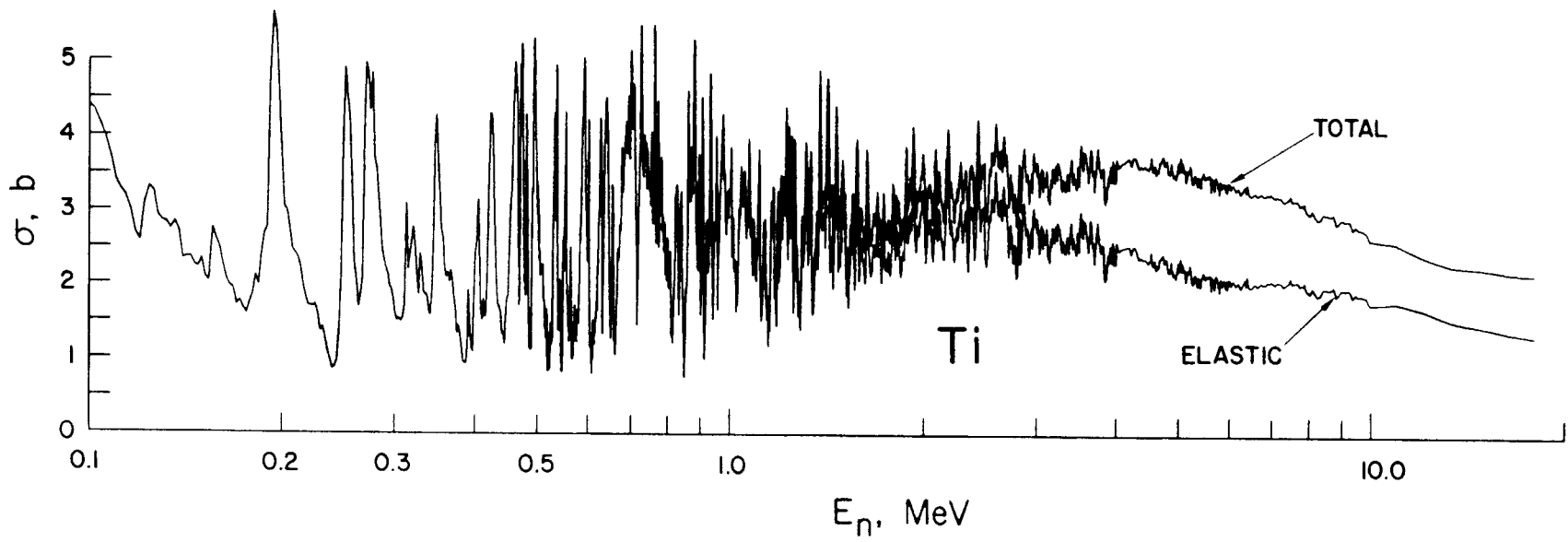


Figure 11

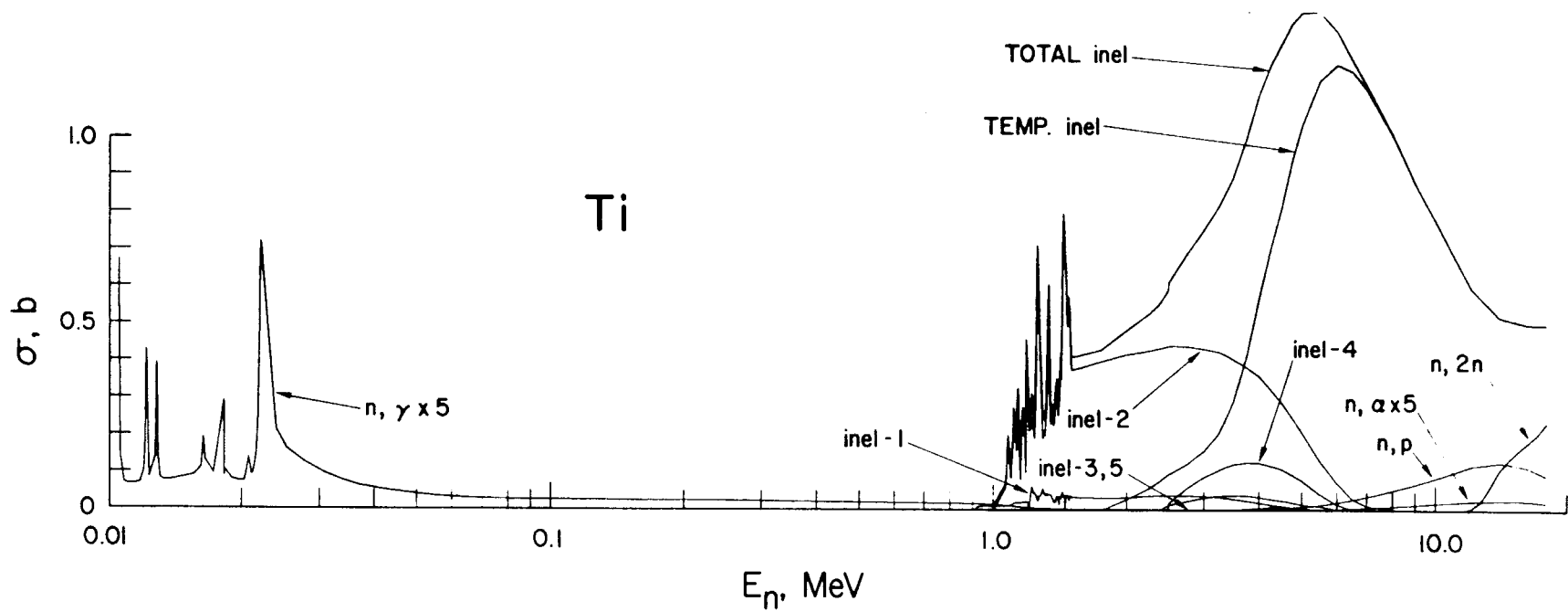


Figure 12